



Year: 2018

Optimized synthesis and indium complex formation with the bifunctional chelator NODIA-Me

Weinmann, Christian ; Holland, Jason P ; Läppchen, Tilman ; Scherer, Harald ; Maus, Stephan ; Stemler, Tobias ; Bohnenberger, Hendrik ; Ezziddin, Samer ; Kurz, Philipp ; Bartholomä, Mark D

Abstract: The bifunctional chelator NODIA-Me holds promise for radiopharmaceutical development. NODIA-Me is based on the macrocycle TACN (1,4,7-triazacyclononane) and incorporates two additional methylimidazole arms for metal chelation and an acetic acid residue for bioconjugation. The original two step synthesis was less than optimal due to low yields and the requirement of semi-preparative RP-HPLC purifications. Here, the overall yield for the preparation of NODIA-Me was improved two- to five-fold via two synthetic routes using different protection/deprotection techniques. This way, it was possible (1) to prepare of NODIA-Me on multi-gram scale and (2) to avoid time-consuming HPLC purifications. Inspired by recent results with nat/68Ga3+, preliminary studies on the radiolabeling properties and complex formation of NODIA-Me with nat/111In3+ were performed. Quantitative radiochemical yields were achieved at ambient temperature providing molar activities of 30 MBq nmol⁻¹, which could be increased to 240 MBq nmol⁻¹ at 95 °C. At r.t., pH 5.5 was optimal for 111In-labeling, but quantitative yields were also achieved in the pH range from 5.5 to 8.2, when the reaction temperature was increased. Stability tests of 111In complexes in vitro revealed high kinetic stabilities in serum and ligand challenge experiments, which is a consequence of the formation of rigid 1 : 1 indium chelates as shown by NMR studies in solution. In summary, the new synthetic routes afford the BFC NODIA-Me in high yields and on large scale. Further, 111In complexation experiments broaden the scope of our chelating system for radiopharmaceutical applications.

DOI: <https://doi.org/10.1039/c8ob01981a>

Posted at the Zurich Open Repository and Archive, University of Zurich

ZORA URL: <https://doi.org/10.5167/uzh-167587>

Journal Article

Accepted Version

Originally published at:

Weinmann, Christian; Holland, Jason P; Läppchen, Tilman; Scherer, Harald; Maus, Stephan; Stemler, Tobias; Bohnenberger, Hendrik; Ezziddin, Samer; Kurz, Philipp; Bartholomä, Mark D (2018). Optimized synthesis and indium complex formation with the bifunctional chelator NODIA-Me. *Organic Biomolecular Chemistry*, 16(40):7503-7512.

DOI: <https://doi.org/10.1039/c8ob01981a>

Optimized Synthesis and Indium complex formation with the bifunctional chelator NODIA-Me

Christian Weinmann^{2,5}, Jason P. Holland⁴, Tilman Läppchen^{2,3}, Harald Scherer⁵, Stephan Maus¹,
Tobias Stemler¹, Hendrik Bohnenberger¹, Samer Ezziddin¹, Philipp Kurz^{5*} and Mark D.
Bartholomä^{1,2*}

¹ Department of Nuclear Medicine, University Hospital Saarland, Saarland University, Kirrbergerstrasse, D-66421, Homburg, Germany

² Department of Nuclear Medicine, University Hospital Freiburg, D-79106, Freiburg, Germany

³ Department of Nuclear Medicine, Inselspital, Bern University Hospital and University of Bern, Freiburgstrasse, CH-3010 Bern, Switzerland

⁴ University of Zurich, Department of Chemistry, Winterthurerstrasse 190, CH-8057, Zurich, Switzerland

⁵ Institute for Inorganic and Analytical Chemistry, Albert-Ludwigs-University Freiburg, Albertstrasse 21, D-79104, Freiburg, Germany

*** Corresponding Authors:**

Dr. Mark D. Bartholomä

E-mail: mark.bartholomae@uks.eu

Prof. Dr. Philipp Kurz

E-mail: philipp.kurz@ac.uni-freiburg.de

Abstract

The bifunctional chelator NODIA-Me holds promise for radiopharmaceutical development. NODIA-Me is based on the macrocycle TACN (1,4,7-triazacyclononane) and incorporates two additional methylimidazole arms for metal chelation and an acetic acid residue for bioconjugation. The original two step synthesis was less than optimal due to low yields and the requirement of semi-preparative RP-HPLC purifications. Here, the overall yield for the preparation of NODIA-Me was improved two- to five-fold via two synthetic routes using different protection/deprotection techniques. This way, it was possible (1) to prepare of NODIA-Me on multi-gram scale and (2) to avoid time-consuming HPLC purifications.

Inspired by recent results with $^{nat/68}\text{Ga}^{3+}$, preliminary studies on the radiolabeling properties and complex formation of NODIA-Me with $^{nat/111}\text{In}^{3+}$ were performed. Quantitative radiochemical yields were achieved at ambient temperature providing molar activities of $\sim 30 \text{ MBq nmol}^{-1}$, which could be increased to $\sim 240 \text{ MBq nmol}^{-1}$ at 95°C . At r.t., pH 5.5 was optimal for ^{111}In -labeling, but quantitative yields were also achieved in the pH range from 5.5 to 8.2, when the reaction temperature was increased. Stability tests of ^{111}In complexes *in vitro* revealed high kinetic stabilities in serum and ligand challenge experiments, which is a consequence of the formation of rigid 1:1 indium chelates as shown by NMR studies in solution. In summary, the new synthetic routes afford the BFC NODIA-Me in high yields and on large scale. Further, ^{111}In complexation experiments broaden the scope of our chelating system for radiopharmaceutical applications.

Key words: NODIA-Me, bifunctional chelator (BFC), Indium-111, prostate-specific membrane antigen (PSMA), single-photon emission computed tomography (SPECT).

Introduction

The majority of radiopharmaceuticals used in nuclear medicine for imaging and therapy are labeled with radioactive metal isotopes. Because of this, targeted radiopharmaceuticals generally comprise a target-specific vector molecule, which carries the radioactivity to the site(s) of interest, and a metal-binding part, a so-called bifunctional chelator (BFC), that (1) is covalently attached to the targeting biomolecule and (2) strongly binds the radiometal ion. However, introduction of a metal chelate is a non-innocent modification that often affects the pharmacological properties of the entire bioconjugate.^{1,2} On the other hand, the dependency of the radiotracer's performance on the chemical structure of the metal chelate also presents an opportunity for chemists to tune the pharmacokinetics of a particular radiopharmaceutical. Tailored chelator design provides control over the metal complex properties such as labeling efficiency and stability but, more importantly, also over the overall charge, lipophilicity and size, thereby serving as valuable tool for radiotracer optimization with regards to target specificity and pharmacokinetics *in vivo*. The important role that the chemical nature of the metal chelate has on the biological performance of targeted radiopharmaceuticals demands continued development and optimization of new BFCs.

We recently developed a chelating system based on the macrocycle TACN (1,4,7-triazacyclononane) that incorporates two or three additional azaheterocycles to provide either a penta- or hexadentate coordination geometry for metal binding. Initial studies focused on the triply substituted compounds NOTI (1,4,7-tris((1*H*-imidazol-2-yl)methyl)-1,4,7-triazonane), NOTI-Me (1,4,7-tris((1-methyl-1*H*-imidazol-2-yl)methyl)-1,4,7-triazonane) and **NOTThia** (1,4,7-tris(thiazol-2-ylmethyl)-1,4,7-triazonane).³ These chelators exhibited excellent complexation properties for the positron- and beta-emitting nuclide $^{64}\text{Cu}^{2+}$, which are a consequence of the pronounced affinity of the borderline Cu^{2+} cation (according to Pearson's hard and soft acids and

bases HSAB principle) to the azaheterocyclic N donors. These findings were also corroborated by Tripier and co-workers, who investigated the complex formation of the TACN based ligand no2th bearing two methylthiazolyl arms with Cu^{2+} and found that the corresponding Cu(II)(no2th) complex was of high thermodynamic and kinetic stability.⁴ Moreover, we showed that TACN derived ligands bearing additional methylimidazole arms can be used for stable complexation of the PET isotope $^{68}\text{Ga}^{3+}$.⁵

More recently, the bifunctional derivative NODIA-Me (2-(4,7-bis((1-methyl-1*H*-imidazol-2-yl)methyl)-1,4,7-triazonan-1-yl)acetic acid) was described, which incorporates an acetic acid group for the covalent attachment of targeting vectors. The applicability of NODIA-Me for the development of ^{68}Ga - and ^{64}Cu -labeled radiopharmaceuticals was subsequently demonstrated by conjugation to a prostate-specific membrane antigen (PSMA) targeting vector.⁵ Small-animal PET imaging and *ex vivo* biodistribution studies of corresponding ^{68}Ga - and ^{64}Cu -labeled NODIA-Me-NaI-Ahx-PSMA conjugates showed specific accumulation in PSMA-positive LNCaP tumors.⁶ Both compounds exhibited rapid renal clearance with low uptake in non-target tissues confirming sufficient stability of ^{68}Ga - and ^{64}Cu (NODIA-Me) chelates *in vivo*. Furthermore, NODIA-Me was recently coupled to the peptide c(RGDfK) for targeting the integrin $\alpha_v\beta_3$ receptor.⁶ The corresponding ^{68}Ga -labeled radiotracer showed low uptake in non-target organs and specific uptake in U-87 MG tumor xenografts in athymic mice, which were clearly visualized by PET.

The initial synthesis of NODIA-Me, however, was suboptimal due to low yields and the need for time-consuming RP-HPLC purifications. Even though NODIA-Me could be obtained in only two reaction steps, the overall yield was only about 20%, and thus, too low for multi-gram scale syntheses. Obviously, these drawbacks demanded optimization of the preparation, which we addressed in the present study.

An ideal BFC should be versatile in terms of complexation to allow its use in combination with various radiometals for different applications. Since our imidazole-type ligands showed excellent complexation properties with the semimetal $^{nat/68}\text{Ga}$, we were also interested in the complex formation of NODIA-Me with the group 13 congener ^{111}In as this might further expand the applicability of our chelating system. The radionuclide ^{111}In decays with a half-life of 2.8 d by electron capture emitting two gamma rays at 171 keV and 245 keV and is widely used in clinics for diagnostic imaging by SPECT or planar scintigraphy. For example, ^{111}In -labeled compounds include antibodies for prostate cancer imaging (ProstaScint®), In(DTPA) for cerebrospinal fluid imaging, In(oxyquinoline) for labeling of white blood cells and In(pentetreotide) for imaging of neuroendocrine tumors (Octreoscan®).⁷⁻¹¹ For information about the coordination chemistry of indium and ligands used for ^{111}In -labeled radiopharmaceuticals the readers are referred to more specialized review articles.^{12, 13}

Experimental

General

Chemicals and solvents of the highest grade commercially available were purchased from Sigma-Aldrich and TCI Europe, and used as received. The precursor Glu-CO-Lys(Ahx)-(tBu)₃ ester was purchased from ABX (Radeberg, Germany) and the macrocycle TACN (1,4,7-triazacyclonane) was obtained from Chematech (Dijon, France). No carrier added [^{111}In]InCl₃ in 0.02 M hydrochloric acid was purchased from Mallinckrodt Pharmaceuticals (Petten, The Netherlands). The bioconjugate NODIA-Me-NaI-Ahx-Lys-CO-Glu (NODIA-Me-NaI-Ahx-PSMA) was prepared as previously described.^{5, 6} NMR spectra were recorded on a Bruker *Avance II WB* (^1H 400 MHz, ^{13}C 101 MHz, ^{14}N 29 MHz, ^{15}N 41 MHz), a Bruker *Avance III HD* (^1H 300 MHz, ^{13}C

75 MHz, ^{14}N 22 MHz, ^{15}N 30MHz) or a Bruker *DPX* (^1H 200 MHz, ^{13}C 50 MHz) at 298 K. Solvents were CDCl_3 or D_2O . Spectra were calibrated on solvent signals (7.260 ppm for CDCl_3 , 4.790 ppm for D_2O).¹⁴ Chemical shifts are given in parts per million (ppm) and are reported relative to trimethylsilane (TMS). Coupling constants are reported in hertz (Hz). The multiplicity of the NMR signals is described as follows: s = singlet, d = duplet, t = triplet, q = quartet, m = multiplet. High resolution mass spectrometry ((+)-HR-ESI-MS) was performed on a Thermo Scientific Exactive mass spectrometer. Reversed-phase high performance liquid chromatography (RP-HPLC) was conducted on an Agilent 1260 Infinity System equipped with an Agilent 1200 DAD UV detector (UV detection at 220 nm) and a Raytest Ramona radiation detector (Raytest GmbH, Straubenhardt, Germany) in series. A Phenomenex Jupiter Proteo (250 x 4.60 mm) column was used for analytical HPLC. The solvent system was A = H_2O (0.1% TFA) and B = acetonitrile (0.1% TFA). The gradient was 0-1 min at 5% B, 1-25 min 5-50% B at a flow rate of 1 mL min^{-1} . Semi-preparative RP-HPLC was performed on a Knauer Smartline 1000 HPLC system in combination with a Macherey Nagel VP 250/21 Nucleosil 120-5 C_{18} column. Conditions were 0-40 min 5-60% B at a flow rate of 12 mL min^{-1} . Samples were lyophilized using a Christ Alpha 1-2 LD plus lyophilizer. For automated reversed-phase flash chromatography, a Biotage *Isolera Four* in combination with a SNAP Ultra C_{18} column (30g) was used. The solvent system was A = H_2O (0.1% TFA) and B = acetonitrile (0.1% TFA). UV detection was set to 220 nm and 240 nm. The gradient used was 0 – 30 mL 0% B, 30 – 120 mL 0-100% B, 120 – 150 mL 100% B at a flow rate of 25 mL min^{-1} . Radioactivity measurements were made by using an Activimeter ISOMED 2010 (Nuklear-Medizintechnik, Dresden, Germany). For accurate quantification of radioactivity, experimental samples were counted for 1 min on a calibrated Perkin Elmer (Waltham, MA) 2480 Automatic Wizard Gamma Counter by using a dynamic energy window of 171 and 245 keV for

¹¹¹In. Radio-TLC strips were analyzed on a Cyclone Plus Storage Phosphor Scanner (PerkinElmer). All instruments measuring radioactivity were calibrated and maintained in accordance with previously reported routine quality-control procedures.¹⁵ A ThermoFisher Heraeus Fresco 21 centrifuge was used for centrifugation. IR spectra were recorded on a *Nicolet iS 10* FT-IR-spectrometer equipped with an ATR unit from ThermoFisher Scientific. Band intensities are described as follows: w = weak, m = medium, s = strong. Elemental analysis was performed using a Vario MICRO cube from Elementar Analysensysteme GmbH.

Synthetic procedures and characterization data of the model compound NODIA-Me-NH-Et (**12**) as well as the metal complexes In-**12** and In-**13** are given in the Supporting Information.

Ligand Syntheses

1,4,7-Tritosyl-1,4,7-triazanonane (1)

Caesium carbonate (9.12 g, 28.0 mmol), dried under vacuum for 1 h at 60 °C, was mixed with *N,N,N'*-tritosyldiethylenetriamine (7.35 g, 13.0 mmol) in dry DMF (80 mL) under argon and allowed to stir for 1.5 h at r.t. (room temperature). To this suspension, a solution of 1,2-bis(tosyloxy)ethane (4.82 g, 13.0 mmol) in dry DMF (30 mL) was added dropwise over 1 h. Stirring was continued for additional 2 d at r.t. The reaction mixture was then poured into water (400 mL) under vigorous stirring resulting in the formation of a colorless precipitate, which was filtered off and dried under vacuum. The colorless solid was suspended in DMF/water (1:1, v/v, 200 mL) and stirred overnight. The crude product was filtered, washed with water (5 x 50 mL), dissolved in dichloromethane and filtered over Celite®. The solvent was removed and the residue taken up in a small volume of dichloromethane (~20 mL). Slow addition of dry ethanol (100 mL) resulted in crystallization of the product. After cooling to 0 °C, crystals were filtered off and dried

under vacuum to give **1** as colorless, crystalline powder (7.40 g, 96%). ¹H NMR (300 MHz, CDCl₃): δ = 7.70 (m, 6H, tosyl), 7.32 (m, 6H, tosyl), 3.42 (s, 12H, macrocycle), 2.43 (s, 9H, tosyl-Me) ppm; ¹³C NMR (75 MHz, CDCl₃): δ = 144.0 (tosyl), 134.7 (tosyl), 130.0 (tosyl), 127.6 (tosyl), 52.0 (macrocycle), 21.7 (tosyl-Me) ppm. HR-ESI-MS calcd m/z for C₂₇H₃₃N₃O₆S₃Na⁺: 614.1423, found: 614.1421. IR (ATR) ν = 3072 (w), 2924 (w), 2851 (w), 1342 (m), 1326 (m), 1154 (s), 1087 (m), 980 (m), 926 (m), 821 (m), 810 (m), 709 (m), 688 (s), 639 (m), 544 (s) cm⁻¹.

1-Tosyl-1,4,7-triazanonane (2)

1,4,7-Tritosyl-1,4,7-triazonane **1** (7.80 g, 13.18 mmol) and phenol (9.41 g, 100.00 mmol) were suspended in a solution of HBr in AcOH (30%, 110 mL) under argon. *Caution*: during the reaction corrosive vapors are released. The mixture was carefully heated to 90 °C for 1 h (*Caution*: gas evolution begins between 60-70 °C), while the reactants completely dissolved. Heating was continued at 90 °C for additional 3 d during which a white precipitate formed (precipitation started after about 2 – 3 h). The reaction mixture was cooled to r.t. and allowed to sit overnight. The formed precipitate was filtered off and washed with diethylether (3 x 20 mL). To this residue, 1.5 M sodium hydroxide was added until complete dissolution (pink solution). The product was extracted from the aqueous phase with chloroform (4 x 15 mL), filtered over Celite[®] and the solvent removed by rotary evaporation. After drying of the product under high vacuum, compound **2** was obtained as a yellowish solid (2.92 g, 78%). ¹H NMR (300 MHz, CDCl₃): δ = 7.68 (m, 2H, tosyl), 7.29 (m, 2H, tosyl), 3.17 (m, 4H, macrocycle), 3.07 (m, 4H, macrocycle), 2.88 (s, 4H, macrocycle), 2.41 (s, 3H, tosyl-Me), 1.74 (s, 2H, NH) ppm. ¹³C NMR (101 MHz, CDCl₃): δ = 143.3 (tosyl), 135.7 (tosyl), 129.8 (tosyl), 127.4 (tosyl), 54.2 (macrocycle), 49.8 (macrocycle), 49.7 (macrocycle), 21.6 (tosyl-Me) ppm. HR-ESI-MS calcd m/z for C₁₃H₂₂N₃O₂S⁺: 284.1427,

found: 284.1430. IR (ATR) ν = 2976 (w), 2946 (w), 2209 (w), 2190 (m), 1717 (w), 1691 (w), 1479 (m), 1450 (m), 1390 (m), 1323 (w), 1230 (m), 1170 (m), 1147 (m), 1112 (w), 998 (m), 921 (s), 782 (m), 685 (m) cm^{-1} .

1-((1-Methyl-1H-imidazol-2-yl)methyl)-4-((1-methyl-4,5-dihydro-1H-imidazol-2-yl)methyl)-7-tosyl-1,4,7-triazanonane (3)

Compound **2** (0.51 g, 1.79 mmol) and 1-methyl-2-imidazolecarboxaldehyde (0.44 g, 4.00 mmol) were dissolved in dry THF (8 mL) under argon. The reaction mixture was stirred at r.t. for 25 h during which a yellow solution formed. Then, sodium triacetoxymethylborohydride (0.46 g, 2.16 mmol) was added in small portions and the resulting suspension stirred for additional 5 h. More sodium triacetoxymethylborohydride (0.45 g, 2.12 mmol) was added in small portions and stirring continued for another 18 h. The reaction was quenched using aqueous hydrochloric acid (1 M, 10 mL) and stirred for additional 30 min. The pH was adjusted to >10 with 40% sodium hydroxide solution resulting in formation of a white precipitate. The aqueous phase was extracted with chloroform (4 x 5 mL) and the combined organic layers washed with water (3 x 10 mL) and brine (10 mL), and dried using anhydrous sodium sulfate. The solvent was removed and the residue taken up in an acetonitrile/water mixture (90:10, 10 mL, both 0.1% TFA). The crude product was further purified by automated flash chromatography. Fractions containing the product were combined, the pH adjusted to pH >10 with aqueous sodium hydroxide solution (10%, ~5 mL) and extracted with chloroform (4 x 10 mL). The chloroform phase was dried with anhydrous sodium sulfate, filtered and the solvent removed under vacuum. After drying under high vacuum, compound **3** was obtained as colorless resin (0.82 g, 98%). ^1H NMR (300 MHz, CDCl_3): δ = 7.56 (m, 2H, tosyl), 7.25 (m, 2H, tosyl), 6.89 (d, J = 1.2 Hz, 2H, imidazole), 6.82 (d, J = 1.2 Hz, 2H, imidazole), 3.71

(s, 4H, CH₂), 3.69 (s, 6H, imidazol-Me), 3.01 (m, 4H, macrocycle), 2.93 (m, 4H, macrocycle), 2.73 (s, 4H, macrocycle), 2.39 (s, 3H, tosyl-Me) ppm. ¹³C NMR (75 MHz, CDCl₃): δ = 145.7 (imidazole), 143.2 (tosyl), 135.5 (tosyl), 129.7 (tosyl), 127.3 (br, tosyl, imidazol), 121.6 (imidazole-CH), 56.4 (macrocycle), 55.0 (macrocycle), 54.5 (CH₂), 51.1 (macrocycle), 33.1 (imidazole-Me), 21.6 (tosyl-Me) ppm. HR-ESI-MS calcd m/z for C₂₃H₃₄N₇O₂S⁺: 472.2489, found: 472.2488. IR (ATR) ν = 2924 (w), 2825 (w), 1498 (m), 1449 (m), 1332 (m), 1283 (m), 1154 (s), 1089 (m), 973 (m), 921 (m), 815 (m), 746 (s), 710 (m), 693 (s), 664 (m), 641 (m), 566 (m), 547 (s) cm⁻¹.

1-((1-Methyl-1H-imidazol-2-yl)methyl)-4-((1-methyl-4,5-dihydro-1H-imidazol-2-yl)methyl)-1,4,7-triazanonane NODI-Me (4)

Removal of the tosyl protecting group was accomplished by heating compound **3** (0.81 g, 1.71 mmol) in concentrated sulfuric acid (15 mL) under argon for 48 h at 110 °C. After cooling to r.t., the reaction mixture was added carefully to ice. The resulting solution was neutralized with sodium hydroxide solution (10%) and the solvent removed by rotary evaporation. The crude product was further purified by automated flash chromatography to give NODI-Me (**4**) · 5 TFA as colorless oil (0.52 g, 34%). ¹H NMR (400 MHz, D₂O, pD < 2): δ = 7.42 (d, *J* = 2.1 Hz, 2H, imidazole), 7.41 (d, *J* = 2.1 Hz, 2H, imidazole), 4.16 (s, 4H, CH₂), 3.82 (s, 6H, imidazole-Me), 3.25 (t, *J* = 5.8 Hz, 4H, macrocycle), 3.01 (t, *J* = 5.8 Hz, 4H, macrocycle), 2.65 (s, 4H, macrocycle) ppm. ¹³C NMR (75 MHz, D₂O, pD < 2): δ = 143.4 (imidazole), 124.4 (imidazole-CH), 119.0 (imidazole-CH), 50.6 (macrocycle), 48.5 (CH₂), 47.6 (macrocycle), 43.9 (macrocycle), 34.7 (imidazole-Me) ppm. ¹⁵N NMR (30 MHz, D₂O, pD < 2): δ = -208 (imidazole), -210 (imidazole-Me), -356 (macrocycle-NH), -349 (macrocycle) ppm. HR-ESI-MS calcd m/z for C₁₆H₂₈N₇⁺: 318.2401, found: 318.2404. IR

(ATR) ν = 2854 (w), 1739 (m), 1669 (s), 1606 (m), 1531 (m), 1461 (m), 1405 (m), 1278 (m), 1128 (s), 1021 (m), 920 (m), 796 (s), 751 (m), 720 (s), 704 (s), 593 (m) cm^{-1} . Elemental analysis calc. C: 35.18%, H: 3.63%, N: 11.05%, found C: 35.75 %, H: 3.99%, N: 10.83%.

Di-tert-butyl (1,4,7-triazanonane-1,4-diyl) bis(carbonate) (5)

To a solution of TACN (3.16 g, 24.47 mmol) in chloroform (80 mL) was added portion-wise BOC-ON (2-(Boc-oxyimino)-2-phenylacetonitrile) (11.98 g, 48.63 mmol) and the mixture was stirred for 3 d at r.t. The solvent was removed and the residue taken up in aqueous sodium hydroxide solution (10%, 32 mL) and diethylether (95 mL). The organic layer was washed with aqueous sodium hydroxide solution (10%, 3 x 16 mL) and water (3 x 16 mL), dried using anhydrous sodium sulfate, filtered and the solvent removed by rotary evaporation. The crude product was purified by silica gel column chromatography (petrol ether/ethylacetate 2:3 followed by ethanol with 1% triethylamine). Fractions containing the product were combined and the solvent removed to give compound **5** as yellow oil (7.10 g, 88%). Several isomers were observed in the NMR measurements. ^1H NMR (400 MHz, CDCl_3): δ = 3.45 (m, 4H, macrocycle), 3.25 (m, 4H, macrocycle), 2.92 (m, 4H, macrocycle), 2.23 (s, 1H, NH), 1.47 (s, 18H, tBu) ppm. ^{13}C NMR (50 MHz, CDCl_3): δ = 156.2, 155.9 (carbonyl), 80.0, 79.9 (tBu), 53.1, 52.5, 52.4, 51.6, 50.6, 50.5, 49.9, 49.7, 48.2, 48.1, 47.7, 47.3 (macrocycle), 28.7 (br, tBu- CH_3) ppm. HR-ESI-MS calcd m/z for $\text{C}_{16}\text{H}_{32}\text{N}_3\text{O}_4^+$: 330.2387, found: 330.2388. IR (ATR) ν = 2974 (w), 2930 (w), 1684 (s), 1461 (m), 1409 (s), 1364 (s), 1245 (s), 1165 (s), 1130 (s), 1071 (w), 1033 (w), 980 (m), 860 (m), 771 (m), 755 (m), 665 (w), 617 (w) cm^{-1} . R_f value (silica plates): 0.05 (PE/EA 2:3), 0.57 (ethanol + 1% Et_3N).

Ethyl 2-(4,7-bis((tert-butoxycarbonyl)oxy)-1,4,7-triazanonan-1-yl)acetate (6)

Compound **5** (0.71 g, 2.16 mmol) and potassium carbonate (1.19 g, 8.62 mmol) were suspended in dry acetonitrile (21.5 mL) under argon. Ethylbromoacetate (0.24 mL, 2.16 mmol) was added dropwise and the mixture was then stirred for 18 h under reflux. The solvent was removed and the residue dissolved in saturated sodium carbonate solution (30 mL). The aqueous phase was extracted with chloroform (3 x 15 mL), the combined organic layers dried using anhydrous sodium sulfate, filtered and the solvent was removed once more by rotary evaporation. The crude product was purified by silica gel column chromatography (petroleum ether/ethylacetate 3:1). Fractions containing the product were combined and the solvent removed to give compound **6** as colorless oil (0.82 g, 91%). Several isomers were observed in the NMR measurements. ¹H NMR (400 MHz, CDCl₃): δ = 4.15 (m, 2H, ethyl-CH₂), 3.45 (m, 4H, macrocycle), 3.42 (s, 2H, CH₂), 3.24 (m, 4H, macrocycle), 2.83 (m, 4H, macrocycle), 1.46 (s, 18H, tBu), 1.26 (m, 3H, ethyl-CH₃) ppm. ¹³C NMR (101 MHz, CDCl₃): δ = 172.2 (br), 172.2, 172.2 (AcOEt-carbonyl), 155.8 (br), 155.8, 155.6 (BOC-carbonyl), 79.6, 79.6, 79.5, 79.5 (tBu), 60.5, 60.4, 60.3, 60.3 (ethyl-CH₂), 56.4 (br, CH₂), 54.5, 53.9, 53.9, 53.7, 51.2, 51.0, 50.9, 50.6, 50.3, 50.0, 49.8, 49.6 (macrocycle), 28.7, 28.7 (tBu-CH₃), 14.5, 14.4 (ethyl-CH₃) ppm. HR-ESI-MS calcd m/z for C₂₀H₃₈N₃O₆⁺: 416.2755, found: 416.2751. IR (ATR) ν = 2975 (w), 2932 (w), 1741 (m), 1686 (s), 1460 (m), 1411 (m), 1365 (m), 1248 (m), 1154 (s), 1098 (m), 1030 (m), 1000 (w), 967 (m), 859 (w), 754 (m) cm⁻¹. R_f value (silica plates): 0.42 (PE/EA 3:1).

Ethyl 2-(1,4,7-triazanonan-1-yl)acetate (7)

Compound **6** (2.21 g, 5.32 mmol) was dissolved in CH₂Cl₂ (6 mL). The solution was cooled with ice and TFA (6 mL) was added dropwise. The reaction mixture was stirred for 2.5 h at r.t. Then,

the solvent was removed. The resulting residue was dissolved in a few drops of water and lyophilized to give the TFA salt of compound **7** · 3 TFA · 4 H₂O as a yellow oil (3.32 g, quant.). ¹H-NMR (300 MHz, D₂O, pD < 2) δ = 4.19 (q, *J* = 7.2 Hz, 2H, ethyl-CH₂), 3.65 (s, 4H, macrocycle), 3.61 (s, 2H, CH₂), 3.31 (m, 4H, macrocycle), 3.09 (m, 4H, macrocycle), 1.23 (t, *J* = 7.2 Hz, 3H, ethyl-CH₃) ppm. ¹³C-NMR (50 MHz, D₂O, pD < 2) δ = 173.9 (carbonyl), 62.3 (ethyl-CH₂), 55.1 (CH₂), 48.5 (macrocycle), 43.9 (macrocycle), 42.6 (macrocycle), 13.2 (ethyl-CH₃) ppm. ¹⁵N-NMR (30 MHz, D₂O, pD < 2) δ = -345 (macrocycle-NH), -363 (macrocycle-AcOEt) ppm. HR-ESI-MS calcd *m/z* for C₁₀H₂₂N₃O₂⁺: 216.1707, found: 216.1704. IR (ATR) ν = 3405 (br, w), 1669 (m), 1435 (w), 1385 (w), 1139 (s), 1029 (m), 941 (w), 841 (m), 799 (m), 783 (m), 723 (m), 704 (m), 598 (m) cm⁻¹. Elemental analysis calc. C: 30.53%, H: 5.12%, N: 6.68%, found C: 31.70%, H: 4.49%, N: 6.61%.

2-(4-((1-Methyl-1H-imidazol-2-yl)methyl)-7-((1-methyl-4,5-dihydro-1H-imidazol-2-yl)methyl)-1,4,7-triazanonan-1-yl)acetic acid NODIA-Me (8)

Route A:

Introduction of the acetic acid arm to give the BFC NODIA-Me **8** was performed as previously reported with a yield of 90%. Characterization was consistent with previously reported data.⁵

Route B:

Compound **7** (2.92 g, 4.65 mmol), 1-methyl- 2-imidazolcarboxaldehyde (1.66 g, 15.08 mmol) and DIPEA (5 mL, 30 mmol) were dissolved in dry THF under argon and heated at 50 °C for 14 h. After cooling to r.t., sodium triacetoxyborohydride (1.53 g, 7.20 mmol) was added in portions and the suspension stirred for 3 h. Then, additional sodium triacetoxyborohydride (1.79 g, 8.44 mmol) was added and stirring continued for additional 3 h. The solvent was removed, the residue taken

up in H₂O/MeCN (0.1% TFA) and purified by flash chromatography. Fractions containing the product were combined and the solvents removed. For hydrolysis of the ester, the residue was refluxed in hydrochloric acid (6 M, 50 mL) for 5 days. After removal of the solvent, the BFC NODIA-Me **8** was obtained as orange oil (2.19 g, 85%). NMR characterization was identical to previously reported NMR data.⁵ HR-ESI-MS calcd m/z for C₁₈H₃₀N₇O₂⁺: 376.2461, found: 376.2459.

Radiolabeling Experiments

¹¹¹In labelling experiments for NODIA-Me-NH-Et ([¹¹¹In]In-12)

An 1 μM stock solution of **12** in the corresponding buffer solution was prepared. For labelling experiments, 33 μL of this stock solution were mixed with 46.5 μL of the corresponding buffer solution (all 0.1 M; NaOAc pH 4.0, NaOAc pH 4.5, NaOAc pH 5.5, MES pH 5.5, HEPES pH 7.4 and NH₄OAc pH 8.2). To these solutions, 1-2 MBq [¹¹¹In]InCl₃ (3 μL) were added to give a total volume of 82.5 μL and a final ligand concentration of 0.4 μM. Reactions were incubated for 15 min at either r.t. or 95 °C. Radiochemical conversion (RCC) was checked by TLC using silica gel microfiber strips (Agilent, iTLC-SG glass microfiber) and DTPA solution (50 mM, pH 7.4). Strips were analyzed by phosphorimaging. For the dilution series, either 16.5, 8.25 or 4.12 μL of ligand stock solution were added to 63, 71.25 or 75.37 μL of ammonium acetate buffer followed by the addition of 1-2 MBq [¹¹¹In]InCl₃ (3 μL). Samples were again incubated for 15 min either at r.t. or 95 °C and the RCC checked by TLC. Each experiment was performed in triplicate. R_f ([¹¹¹In]In-**12**) = 0-0.1, R_f ([¹¹¹In]In-DTPA) = 0.9-1.0.

¹¹¹In labelling experiments for NODIA-Me-NaI-Ahx-PSMA ([¹¹¹In]In-13)

An aliquot of a stock solution of the bioconjugate **13** ($2\ \mu\text{g}\ \mu\text{L}^{-1}$) in water was 1000-fold diluted in the corresponding labelling buffer (all 0.1 M; NaOAc pH 4.0, NaOAc pH 4.5, NaOAc pH 5.5, MES pH 5.5, HEPES pH 7.4, HEPES pH 8.2 and NH_4OAc pH 8.2) followed by the addition of $\sim 1\text{-}2\ \text{MBq}\ [^{111}\text{In}]\text{InCl}_3$. In a typical labelling experiment, $17\ \mu\text{L}$ ($\sim 0.033\ \text{nmol}$) of the diluted stock solution of **13** were added to $75\ \mu\text{L}$ labelling buffer followed by $8\ \mu\text{L}$ ($\sim 1\text{-}2\ \text{MBq}$) $[^{111}\text{In}]\text{InCl}_3$. After brief mixing, samples were either incubated at r.t. or $95\ ^\circ\text{C}$ for 15 minutes. Analysis was initially performed by analytical RP-HPLC and the RCC was determined as described for **12**. No differences between the HPLC and TLC analyzed samples were observed so that determination was continued by TLC. Each experiment was performed at least in triplicate. $R_f([^{111}\text{In}]\text{In-13}) = 0\text{-}0.1$, $R_f([^{111}\text{In}]\text{In-DTPA}) = 0.9\text{-}1.0$. RP-HPLC (analytical, radioactivity detector): $t_R([^{111}\text{In}]\text{In-13}) = 17:46\ \text{min}$.

In Vitro Characterization

Lipophilicity ($\log D_{\text{oct/PBS}}$) measurements

For the determination of the partition coefficient, $\sim 0.4\ \text{MBq}$ of $[^{111}\text{In}]\text{In-13}$ in saline ($20\ \mu\text{L}$) was added to a pre-saturated mixture of phosphate buffered saline pH 7.4 (PBS) ($480\ \mu\text{L}$) and *n*-octanol ($500\ \mu\text{L}$). Samples were shaken for 1 h at r.t. For separation, the samples were centrifuged at $21,100\ \text{g}$ for 5 min. From each phase, $50\ \mu\text{L}$ were transferred into counting tubes, and samples were counted using a Perkin Elmer gamma counter. The experiment was performed in triplicate.

DTPA challenge experiments

$0.2\text{-}0.4\ \text{MBq}$ ($10\ \mu\text{L}$) of $[^{111}\text{In}]\text{In-13}$ were added into $200\ \mu\text{L}$ of DTPA (diethylenetriamine pentaacetic acid) ($50\ \text{mM}$, pH 7.4) and stored at r.t. At selected time points, $20\ \mu\text{L}$ samples were drawn

and analyzed by analytical RP-HPLC. The percentage of intact ^{111}In -**13** was calculated from the HPLC chromatograms. The experiment was performed in triplicate.

Serum stability measurements

0.5–1 MBq (50 μL) of [^{111}In]In-**13** were added to human serum (1 mL, human male AB plasma, Sigma-Aldrich), which was pre-equilibrated at 37 °C in a cell incubator for 1 h. Samples were vortexed and stored at 37 °C. At selected time points, 100 μL aliquots were taken and serum proteins were removed by centrifugation (4,000 g for 5 min at 4 °C) using molecular weight cutoff filter tubes (30 kDa). The filter was then washed twice with 100 μL PBS with additional centrifugation steps. For determination of protein bound fraction, the filters and the filtrates were transferred into counting tubes, and samples were measured using a Perkin Elmer gamma counter. A sample of the filtrate was kept on ice until HPLC analysis. The percentage of intact ^{111}In -**13** was calculated from the HPLC chromatograms. The experiment was performed in triplicate.

Competitive binding assay

PSMA-positive LNCaP cells (ATCC, Manassas, VA, USA) were cultured at 37 °C under a 5% CO_2 atmosphere (RPMI Medium 1640 GlutaMAX containing 10% FBS, 1% 100 U mL^{-1} penicillin and 100 $\mu\text{g mL}^{-1}$ streptomycin, 1% sodium-pyruvate 1 mM, 1% L-glutamin 2 mM). The binding affinity of the bioconjugate **13** and the corresponding In-**13** was determined using a cell-based competitive binding assay with ^{68}Ga -labelled PSMA-HBED-CC (DKFZ-PSMA-11) according to the literature with minor modifications.¹⁶ Briefly, each compound at different concentrations (0 – 10,000 nM) was incubated for 1 h at 37 °C with 0.15 nM [^{68}Ga]Ga-PSMA-HBED-CC together with 2×10^5 LNCaP cells per well. After incubation, cells were washed three times with ice-cold

PBS and cell-associated activity recovered by addition of 1 M NaOH. Radioactivity was measured by a Perkin Elmer gamma counter and data fitted using non-linear regression (GraphPad Prism). Experiments were performed two times in triplicate.

Results and Discussion

Ligand Syntheses

In order to improve the overall yield for the synthesis of NODIA-Me and to avoid the cumbersome purification by semi-preparative RP-HPLC, two synthetic strategies using different protecting group techniques were investigated (Scheme 1). Route A starts with the commercially available and cost-effective starting materials *N,N',N''*-tritosyldiethylenetriamine and 1,2-bis(tosyloxy)ethane enabling the simultaneous build-up and protection of the TACN ring in 96% yield (Scheme 1A).¹⁷ The triply tosyl-protected TACN derivative **1** was then selectively deprotected in a HBr/AcOH mixture to give the single-protected compound **2** in 78% yield. The mono-protected TACN **2** is not soluble in the reaction mixture and precipitates with progression of the reaction. The intermediate **2** was consequently isolated by filtration. Introduction of the methylimidazole residues was accomplished by reductive amination with minor modifications to reported methods producing the intermediate **3** in an almost quantitative yield of 98%.³ NODI-Me **4** was obtained in 34% yield after removal of the final tosyl protecting group by refluxing compound **3** in concentrated sulfuric acid for 48 h. We did not attempt to optimize the conditions of this deprotection step because in spite of these harsh reaction conditions, the overall yield for NODI-Me was approximately doubled (25% vs. 14%) through the use of this protection-deprotection approach, thereby eliminating the need for RP-HPLC purification. Introduction of the acetic acid arm to obtain the BFC NODIA-Me **8** was accomplished by reductive amination using

glyoxylic acid as previously reported with an overall yield of 22%.⁵ This is a ~two-fold improvement over the initial two-step synthesis. The advantage of Route A is the cost-effective and straightforward access to the mono-protected TACN ring. However, the harsh reaction conditions for removal of the final tosyl group from **3** limit its use to acid resistant substituents. Future work will focus on the optimization of the final deprotection step and might result in a further improvement of the overall yield.

In order to circumvent the need for harsh deprotection conditions, another synthesis route was investigated as a possible alternative (Scheme 1B). In this case, the TACN ring was converted into its di-BOC protected derivative **5** using BOC-ON (2-(Boc-oxyimino)-2-phenylacetonitrile) according to the literature.¹⁸ The acidic acid residue was then introduced to the di-BOC protected TACN derivative **5** via nucleophilic substitution using ethylbromoacetate and potassium carbonate to give compound **6** in 91% yield. BOC protection resulted in formation of different isomers that were identified by NMR. Removal of the BOC protecting groups was accomplished by reaction with TFA in CH₂Cl₂ to provide the intermediate **7** in quantitative yield. Once again, the introduction of the methylimidazole residues was achieved by reductive amination using 1-methyl-2-imidazolecarboxaldehyde and sodium triacetoxyborohydride. Hydrolysis of the ethyl ester was accomplished by refluxing in 6 M hydrochloric acid for 5 days to obtain NODIA-Me **8** in 85% yield. The overall yield for this 4-step synthesis was 68%, which marks a ~five-fold improvement compared to the initial synthesis. Furthermore, hydrolysis of the ethyl ester of **6** can alternatively be performed prior to the introduction of the imidazole substituents with no significant differences in overall yield. Simultaneous removal of the BOC groups and hydrolysis of the ethyl ester was achieved by refluxing compound **6** in 6 M hydrochloric acid followed by the introduction of the

imidazole substituents. This way, acid sensitive substituents can be introduced after preparation of the mono acetic acid derivative.

Overall, two novel synthetic routes for the preparation of the BFC NODIA-Me **8** with improved overall yields have been developed. While route A is appealing due to the cost-effective build-up of the TACN ring, its major drawback is the removal of the final tosyl protecting group, which could only be achieved in relatively low yield resulting in a decrease of the overall yield. The harsh reaction conditions also limit this pathway to acid-resistant substituents. On the other hand, route B provided NODIA-Me **8** in a significantly improved overall yield and allows the introduction of acid-sensitive substituents for future applications. A minor drawback of route B is that this route does not include the preparation of the costly TACN macrocycle.

¹¹¹Indium radiolabeling and stability experiments

The complex formation of the imidazole-type ligands NOTI-Me and NODIA-Me with the important PET isotope $^{68}\text{Ga}^{3+}$ was recently described.⁵ We found that the borderline N donors of the imidazoles (according to Pearson's HSAB principle) in combination with the TACN moiety are well suited for complexation of the hard Lewis acid Ga^{3+} . Motivated by these results, we were also interested in the complex formation of NODIA-Me with $^{\text{nat}/111}\text{In}^{3+}$ as this might further expand the applicability of our chelating system for radiopharmaceutical development.

The most important requirement for a BFC is its ability to complex the radiometal of interest. Labeling properties of the model chelator NODIA-Me-NH-Et **12**, in which the acetic acid was transformed into the corresponding ethylamide to mimic conjugation to a targeting vector, as well as the PSMA-targeting bioconjugate **13** with the gamma-emitter $^{111}\text{In}^{3+}$ were therefore studied in detail (Scheme 3). In order to determine the optimal labeling conditions in terms of molar activity,

time, temperature and pH, initial experiments were performed with the model compound NODIA-Me-NH-Et **12**. First, the minimum amount of **12** to achieve quantitative radiochemical conversion (RCC) at pH 5.5 in acetate buffer at r.t. and 95 °C was determined. These conditions have been successfully applied for ^{111}In -labeling of other BFCs such as DPTA, DOTA and NOTA.¹⁹⁻²² As can be seen from the results given in Figure 1A, a chelator concentration of 0.4 μM was necessary to obtain quantitative RCCs at r.t., which corresponded to a molar activity of $A_m = \sim 30 \text{ MBq nmol}^{-1}$. With decreasing ligand concentrations, the RCC decreased subsequently at ambient temperature. However, heating to 95 °C resulted in quantitative RCCs at ligand concentrations as low as 0.05 μM corresponding to a molar activity of $A_m = \sim 240 \text{ MBq nmol}^{-1}$. Next, the effect of the pH on the RCC of NODIA-Me-NH-Et **12** (Figure 1B) was studied. With the exception of pH 4.0, quantitative RCCs were obtained over a pH range of 5.5 to 8.2 at r.t. and 95 °C using a ligand concentration of 0.4 μM .

Since the presence of a targeting vector can have an impact on the radiolabeling properties, additional labeling experiments using the PSMA-targeting bioconjugate **13** were performed. First, the optimal pH for radiolabeling of the PSMA-conjugate **13** was determined at a conjugate concentration of 0.33 μM . At 95 °C, quantitative RCCs in molar activities of $\sim 30 \text{ MBq nmol}^{-1}$ were obtained over the entire investigated pH range from 4.0 to 8.2 (Figure 1C). To the contrary, significant differences in RCC were found at r.t. Similar to the ligand **12**, the optimal pH for radiolabeling of the bioconjugate **13** was pH 5.5 but the RCC decreased significantly at r.t. at pH values below and above pH 5.5. Interestingly, the nature of the buffer salt (sodium acetate *versus* MES) did not impact the RCC at pH 5.5, while at pH 8.2 the difference in RCCs between HEPES and sodium acetate was $\sim 25\%$.

Besides the labeling efficiency, the stability/inertness of the radiometal complex is of importance for radiopharmaceutical applications. Hence, the stability of ^{111}In -labeled **13** was assessed in ligand challenge and serum stability measurements. For the ligand exchange study, an aliquot of ^{111}In -**13** was incubated in $\sim 3 \times 10^6$ -fold molar excess of DTPA at r.t. and samples were analyzed at selected time points by RP-HPLC. Corresponding chromatographic data is given in the Supporting Information. No exchange was noted for up to 24 h confirming the formation of a stable ^{111}In -**13** complex under these conditions. This finding was furthermore corroborated by serum stability measurements, in which ^{111}In -**13** remained intact to >99% for up to 24 h underscoring the stability of the radiometal complex. The protein bound fraction of ^{111}In -**13** was with $30.3 \pm 3.9\%$ comparable to that of previously reported conjugates ^{64}Cu -**13**, ^{68}Ga -**13** and ^{68}Ga -PSMA-HBED-CC.⁶ The octanol/PBS partition coefficient $\log D_{\text{oct/PBS}}$ of ^{111}In -**13** was determined to -3.57 ± 0.01 making it slightly more lipophilic than its ^{64}Cu - and ^{68}Ga -labeled counterparts with $\log D_{\text{oct/PBS}}$ values of -3.99 ± 0.05 and -4.27 ± 0.08 , respectively.⁶

Complex formation of NODIA-Me-NH-Et with In^{3+}

To better understand the encouraging results of the labeling and stability experiments, the complex formation of NODIA-Me-NH-Et **12** with $^{\text{nat}}\text{In}^{3+}$ was investigated. To gain further insights into the structural features of corresponding metal complexes, a series of 1D- and 2D-NMR measurements of **12** were performed in aqueous medium. Figure 2 shows a comparison between the proton NMR spectra of metal-free **12** and **In-12**. A detailed overview of the proton and carbon NMR resonances is given in the Supporting Information. In these NMR studies, a similar trend was observed as seen for the previously described $\text{Ga}(\text{NODIA-Me-NH-Me})$ complex.⁵ Upon metal coordination, the proton resonances of the TACN macrocycle are deshielded compared to the free

ligand confirming coordination to the metal center. The diastereotopic ring protons of TACN exhibit an AA'BB' multiplet confirming a slow TACN ring conformational interconversion for In-**12** comparable to the In(NOTA) complex.²³ Similar to studies on Ga(NODIA-Me-NH-Me), the imidazole protons are shifted to higher field, which is caused by the anisotropic effect of the aromatic imidazole rings. The protons of the CH₂ groups of the methylimidazole arms are not chemically equivalent and hence show an AB coupling pattern, which is consistent with an inert binding of the imidazole N donors to the metal center. In contrast, the methylene protons of the acetic acid arms of In(NOTA) resonated as singlets being representative for a short lifetime of corresponding In-O bonds.²³ The CH₂ protons of the acetic acid arm show a singlet indicating that the amide function is most likely not involved in metal binding. However, from these results a fast exchanging coordination via the carbonyl-O or amide-NH in solution cannot entirely be excluded. Interestingly, corresponding protons are also shielded, which is in contrast to the Ga(NODIA-Me-NH-Me) complex. Altogether, the proton NMR of In-**12** is consistent with formation of a rigid 1:1 chelate with a slow conformational interconversion of the macrocycle and inert In-N bonds to the imidazole arms.

Trivalent indium ions can form complexes with coordination numbers four to eight and the majority of ligands used for radiopharmaceuticals form six-, seven- and eight-coordinate complexes.¹² For TACN derived ligands coordination numbers 6 and 7 have been reported. For example, X-ray analysis of In(NOTA) showed formation of a heptacoordinate complex with a pentagonal bipyramidal geometry with the coordination sphere being formed by six donor atoms provided by NOTA and an additional coordinated chloride anion.²³ However, in aqueous solution NMR spectral data suggested a time-averaged six-coordinate C₃ symmetric In(NOTA) complex.²⁴ X-ray analysis of structurally related In-(*R,R,R*)-1,4,7-tris(2'-methylcarboxymethyl)-

triazacyclononane complex revealed a distorted trigonal prismatic coordination sphere.²⁵ Six-coordinate In complexes have also been reported for a tris(phenylphosphinate)- as well as a tris(mercaptoethyl)-armed TACN derivative.^{26, 27} In case of In(NODIA-Me-NH-Et), formation of a seven- or even eight-coordinate complex with additional weakly bound monodentate ligands such as H₂O, hydroxide or chloride, etc. cannot entirely be excluded even though coordination of such ligands could not be shown by NMR. Additional IR spectroscopy of **12** and In-**12** to elucidate further the coordination environment of the chelate was not conclusive due to overlapping signals in the regions of interest. Mass spectrometry of In-**12** and In-**13** only showed m/z consistent of metal chelates without the presence of additional ligands. Moreover, an exchange between monodentate ligands, as reported by our group for a similar ⁶⁸Ga-labeled NODIA-Me-Ahx-PSMA conjugate⁵, was not noted in any experiments of ^{nat/111}In-**12** or ^{nat/111}In-**13**. From these data, it can be concluded that NODIA-Me forms an In complex of uniform composition. Chemically plausible is either a six-coordinate complex involving donation from the amide group, or a seven/eight-coordinate complex with additional monodentate ligands, most likely H₂O molecules.

Competitive binding assay

To demonstrate the applicability of the In(NODIA-Me) complex for biological applications, preliminary biological testing was performed using the bioconjugate **13**. Corresponding ⁶⁴Cu- and ⁶⁸Ga-labeled NODIA-Me-NaI-Ahx-PSMA conjugates were recently evaluated by our group.⁶ For comparison and to study the influence of the indium complex on biological properties, the binding affinities of **13** and In-**13** were determined in competitive binding assays on PSMA-positive LNCaP cells as previously described.⁶ A graphical representation of corresponding IC₅₀ curves is given in Figure 3. Coordination of the In³⁺ cation resulted in a ten-fold decrease in affinity *versus*

the metal-free conjugate **13** with IC_{50} values of 2539 ± 100 nM and 233 ± 10 nM, respectively. IC_{50} values of the previously reported counterparts Cu-**13** and Ga-**13** were determined to 681 ± 7 nM and 176 ± 10 nM, respectively. The BFC NODIA-Me **8** does not possess any charge compensating donor atoms resulting in metal complexes with a positive overall charge. Since both conjugates form complexes with two-fold positive overall charge, in case of the Ga complex either a hydroxide or chloride anion occupy the remaining coordination site, we attributed the lower affinity of Cu-**13** *versus* Ga-**13** to differences in complex size and polarity. The In^{3+} cation is sterically more demanding due to its larger ionic radius compared to Cu^{2+} and Ga^{3+} making the corresponding complex obviously too bulky for optimal binding to PSMA. Overall, the results of the competitive cell binding assay did not justify testing of [^{111}In]In-**13** in animals.

Conclusions

In this work, two novel synthesis strategies for NODIA-Me were introduced. In both cases using different protection/deprotection techniques, the overall yield was improved. While one synthetic route provided cost-effective and straightforward access to the mono-protected TACN ring, the relatively low yield for the removal of the final tosyl protecting group resulted only in a two-fold increase in overall yield. In addition, the harsh deprotecting conditions required for the removal of the final tosyl group limits the application of this route to acid resistant substituents. Via the second strategy using BOC protecting groups, the overall yield was significantly improved five-fold allowing the preparation of NODIA-Me in multi-gram scale. Importantly, this pathway is also compatible with the introduction of acid-sensitive substituents for future applications. Both pathways avoid the cumbersome and time-consuming purification by RP-HPLC.

In the second part of this work, preliminary studies on the complex formation of NODIA-Me with $^{nat/111}\text{In}$ were performed. The BFC NODIA-Me was successfully labeled with the gamma-emitter ^{111}In at ambient temperature in high radiochemical yield and purity as well as moderate to high molar activities. Furthermore, the corresponding ^{111}In complex was highly stable *in vitro* as shown by human serum stability and ligand challenge experiments. The model compound NODIA-Me-NH-Et forms rigid 1:1 chelates with In^{3+} , which is in accordance with our previous report on a similar complex of its group 13 congener Ga^{3+} . The indium-labeled NODIA-Me-NaI-Ahx-PSMA bioconjugate was also tested in competitive cell binding experiments. In comparison to the copper- and gallium-labeled counterparts, the binding affinity was very low being a consequence of the rather bulky indium complex, which obviously avoids optimal accommodation of the In-labeled bioconjugate to PSMA. Summarizing, the BFC NODIA-Me is now accessible in large scale. The results of ^{111}In -labelling and *in vitro* stability experiments are encouraging and support future development of ^{111}In -labeled radiopharmaceuticals based on our chelating system for evaluation with more appropriate targeting vectors *in vivo*.

Acknowledgements

JPH thanks the Department of Nuclear Medicine, University Hospital Freiburg, the German Cancer Consortium (DKTK), the German Cancer Research Center (DKFZ), the Swiss Cancer League (Krebsliga Schweiz; KLS-4257-08-2017), the Swiss National Science Foundation (SNSF Professorship PP00P2_163683), the European Research Council (ERC-StG-2015, NanoSCAN – 676904), and the University of Zurich for financial support. MDB thanks the Chemistry Department of the Albert-Ludwigs-University Freiburg (Germany) for its support, in particular Christoph Warth for MS measurements. MDB also thanks the Fonds der Chemischen Industrie for funding.

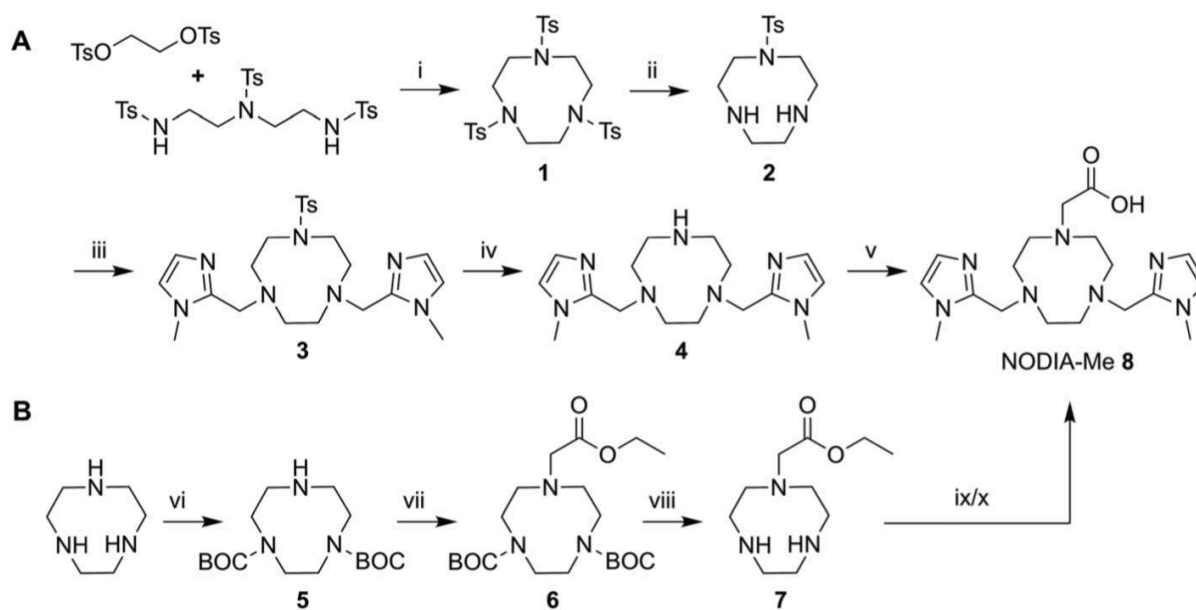
References

1. B. M. Zeglis, J. L. Houghton, M. J. Evans, N. Viola-Villegas and J. S. Lewis, *Inorg. Chem.*, 2014, **53**, 1880-1899.
2. M. D. Bartholomä, *Inorg. Chim. Acta*, 2012, **389**, 36-51.
3. C. Gotzmann, F. Braun and M. D. Bartholomä, *RSC Advances*, 2016, **6**, 119-131.
4. M. Le Fur, M. Beyler, N. Le Poul, L. M. Lima, Y. Le Mest, R. Delgado, C. Platas-Iglesias, V. Patinec and R. Tripier, *Dalton Trans.*, 2016, **45**, 7406-7420.
5. A. Schmidtke, T. Läppchen, C. Weinmann, L. Bier-Schorr, M. Keller, Y. Kiefer, J. P. Holland and M. D. Bartholomä, *Inorg. Chem.*, 2017, **56**, 9097-9110.
6. T. Läppchen, J. P. Holland, Y. Kiefer and M. D. Bartholomä, *EJNMMI Radiopharm. Chem.*, 2018, **3**, 6.
7. S. S. Taneja, *Reviews in Urology*, 2004, **6**, S19-S28.
8. T. M. O'Dorisio and L. B. Anthony, *Front. Horm. Res.*, 2015, **44**, 177-192.
9. W. H. Simon and W. S. Joseph, *Clin. Podiatr. Med. Surg.*, 1988, **5**, 329-340.
10. P. J. Jeffery, S. Sostre, L. R. Scherer, W. Kasecamp and E. E. Camargo, *Eur. J. Nucl. Med.*, 1990, **17**, 365-368.
11. S. S. Taneja, *Rev. Urol.*, 2004, **6 Suppl 10**, S19-28.
12. T. J. Wadas, E. H. Wong, G. R. Weisman and C. J. Anderson, *Chem. Rev.*, 2010, **110**, 2858-2902.
13. S. Liu, *Adv Drug Deliv Rev*, 2008, **60**, 1347-1370.
14. H. E. Gottlieb, V. Kotlyar and A. Nudelman, *J. Org. Chem.*, 1997, **62**, 7512-7515.
15. P. Zanzonico, *J. Nucl. Med.*, 2009, **49**, 1114-1131.
16. M. Benešová, U. Bauder-Wüst, M. Schäfer, K. D. Klika, W. Mier, U. Haberkorn, K. Kopka and M. Eder, *J. Med. Chem.*, 2016, **59**, 1761-1775.
17. D. A. Valyaev, S. Clair, L. Patrone, M. Abel, L. Porte, O. Chuzel and J.-L. Parrain, *Chemical Science*, 2013, **4**, 2815-2821.
18. H. S. Chong, X. Ma, T. Le, B. Kwamena, D. E. Milenic, E. D. Brady, H. A. Song and M. W. Brechbiel, *J. Med. Chem.*, 2008, **51**, 118-125.
19. Z. Varasteh, I. Velikyan, G. Lindeberg, J. Sörensen, M. Larhed, M. Sandström, R. K. Selvaraju, J. Malmberg, V. Tolmachev and A. Orlova, *Bioconjugate Chem.*, 2013, **24**, 1144-1153.
20. K. G. Andersson, M. Rosestedt, Z. Varasteh, M. Malm, M. Sandstrom, V. Tolmachev, J. Lofblom, S. Stahl and A. Orlova, *Oncol. Rep.*, 2015, **34**, 1042-1048.
21. J. Malmberg, A. Perols, Z. Varasteh, M. Altai, A. Braun, M. Sandstrom, U. Garske, V. Tolmachev, A. Orlova and A. E. Karlstrom, *Eur. J. Nucl. Med. Mol. Imaging*, 2012, **39**, 481-492.
22. M. Brom, L. Joosten, W. J. G. Oyen, M. Gotthardt and O. C. Boerman, *EJNMMI Research*, 2012, **2**, 4-4.
23. C. J. Broan, J. P. L. Cox, A. S. Craig, R. Katakya, D. Parker, A. Harrison, A. M. Randall and G. Ferguson, *J. Chem. Soc. Perk. 2*, 1991, DOI: 10.1039/P29910000087, 87-99.
24. A. S. Craig, I. M. Helps, D. Parker, H. Adams, N. A. Bailey, M. G. Williams, J. M. A. Smith and G. Ferguson, *Polyhedron*, 1989, **8**, 2481-2484.
25. R. C. Matthews, D. Parker, G. Ferguson, B. Kaitner, A. Harrison and L. Royle, *Polyhedron*, 1991, **10**, 1951-1953.

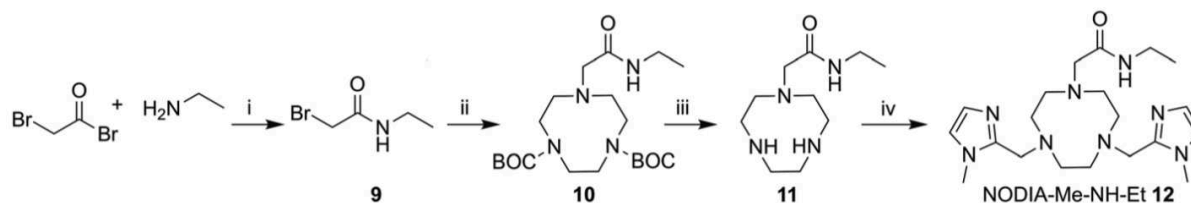
26. E. Cole, R. C. B. Copley, J. A. K. Howard, D. Parker, G. Ferguson, J. F. Gallagher, B. Kaitner, A. Harrison and L. Royle, *J Chem Soc Dalton*, 1994, DOI: DOI 10.1039/dt9940001619, 1619-1629.
27. U. Bossek, D. Hanke, K. Wieghardt and B. Nuber, *Polyhedron*, 1993, **12**, 1-5.

Figure, Scheme and Table Legends

Scheme 1. Synthesis routes for the BFC NODIA-Me **8**. Route A: i) Cs_2CO_3 , DMF, 2 d, 96%; ii) phenol, HBr/AcOH , 3 d, 90 °C, 78%; iii) 1-methyl-2-imidazolecarboxaldehyde, $\text{NaBH}(\text{OAc})_3$, THF, 24 h, 98%; iv) H_2SO_4 conc., 110 °C, 48 h, 34%; v) glyoxylic acid, $\text{NaBH}(\text{OAc})_3$, 1,2-dichloroethane, 16 h, 90%. Route B: vi) BOC-ON, CHCl_3 , 3 d, 88%; vii) K_2CO_3 , ethylbromoacetate, MeCN, reflux, 18 h, 91%; viii) CH_2Cl_2 , TFA, 0 °C to r.t., 2.5 h, quantitative; ix) 1-methyl-2-imidazolecarboxaldehyde, DIPEA, $\text{NaBH}(\text{OAc})_3$, THF, 50 °C, 20 h; x) 6 M HCl_{aq} , reflux, 5 d, 85% over two steps



Scheme 2. Synthesis of model compound NODIA-Me-NH-Et **12**. i) K_2CO_3 , CH_2Cl_2 , 17 h, 61%; ii) K_2CO_3 , **5**, MeCN, 18 h, 89%; iii) TFA, CH_2Cl_2 , 2 h, 73%; iv) 1-methyl-2-imidazolecarboxaldehyde, $\text{NaBH}(\text{OAc})_3$, THF, 22 h, 62%



Scheme 3. Model compound NODIA-Me-NH-Et **12** and PSMA-targeting bioconjugate NODIA-Me-Nal-Ahx-PSMA **13**

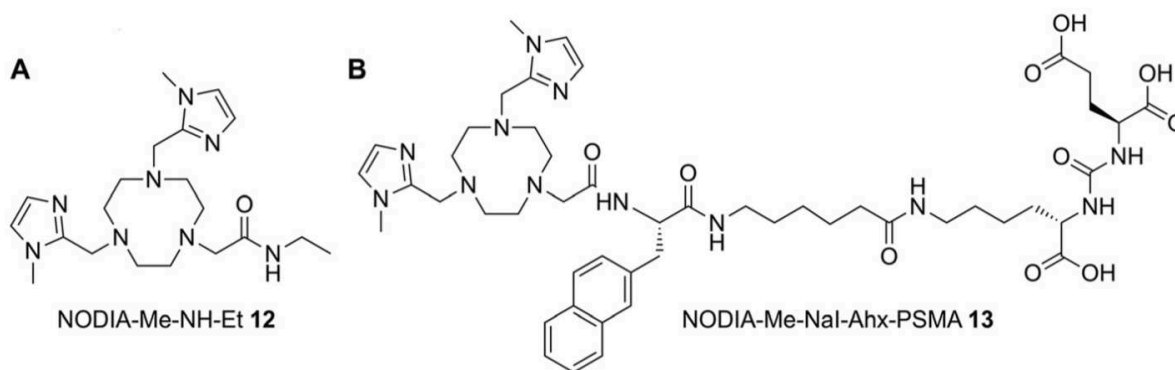


Figure 1. ^{111}In -labeling experiments at r.t. / 95 °C and various pHs (all buffers 0.1 M). A) NODIA-Me-NH-Et **12** at various ligand concentrations at pH 5.5 (NaOAc 0.1 M); B) NODIA-Me-NH-Et **12** at different pH values ($c(\text{L}) = 0.4 \mu\text{M}$); C) NODIA-Me-NaI-Ahx-PSMA **13** at different pH values ($c(\text{L}) = 0.33 \mu\text{M}$)

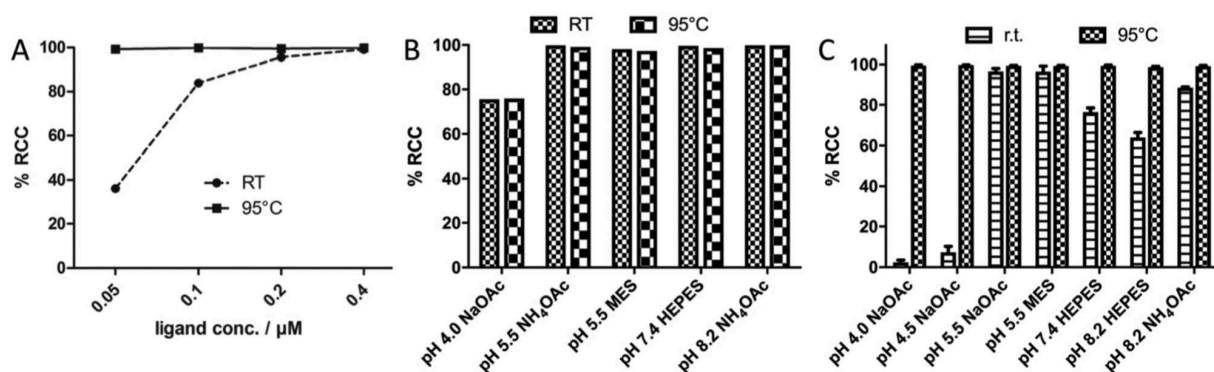


Figure 2. Proton NMR spectra of (A) complex In-**12** and (B) metal-free NODIA-Me-NH-Et **12**

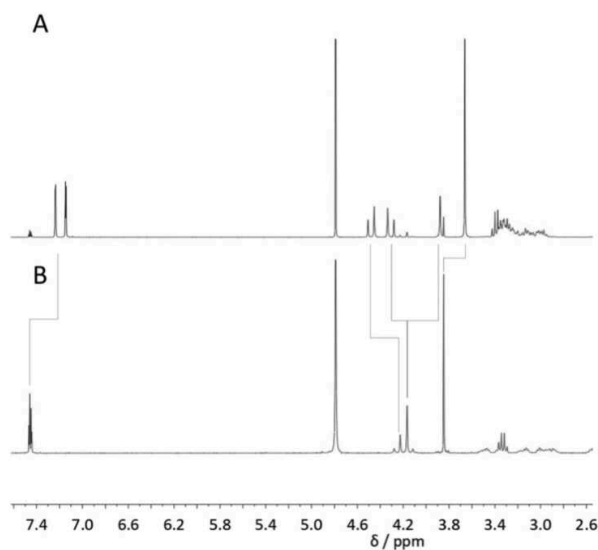


Figure 3. Determination of binding affinity of **13** and In-**13** by competitive titration on LNCaP cells using [^{68}Ga]Ga-PSMA-HBED-CC as radioligand

